Computational and Structural Biotechnology Journal 23 (2024) 2230–2239

Contents lists available at ScienceDirect

Computational and Structural Biotechnology Journal

journal homepage: www.elsevier.com/locate/csbj

Aluminum chloride and D-galactose induced a zebrafish model of Alzheimer's disease with cognitive deficits and aging

Li Luo [a], Tao Yan [b], Le Yang [b,*], Minggao Zhao [a,*]

[a] Institute of Medical Research, Northwestern Polytechnical University, Xi'an, Shaanxi 710072, China
[b] Precision Pharmacy & Drug Development Center, Department of Pharmacy, Tangdu Hospital, Air Force Medical University, Xi'an 710038, China

ARTICLE INFO

Keywords:
Alzheimer's disease
Zebrafish
Aluminum chloride
D-galactose
High-throughput screening

ABSTRACT

Alzheimer's disease (AD) is an age-related neurodegenerative disorder. Transgenic and pharmacological AD models are extensively studied to understand AD mechanisms and drug discovery. However, they are time-consuming and relatively costly, which hinders the discovery of potential anti-AD therapeutics. Here, we established a new model of AD in larval zebrafish by co-treatment with aluminum chloride ($AlCl_3$) and D-galactose (D-gal) for 72 h. In particular, exposure to 150 μM $AlCl_3$ + 40 mg/mL D-gal, 200 μM $AlCl_3$ + 30 mg/mL D-gal, or 200 μM $AlCl_3$ + 40 mg/mL D-gal successfully induced AD-like symptoms and aging features. Co-treatment with $AlCl_3$ and D-gal caused significant learning and memory deficits, as well as impaired response ability and locomotor capacity in the plus-maze and light/dark test. Moreover, increased acetylcholinesterase and β-galactosidase activities, β-amyloid 1–42 deposition, reduced telomerase activity, elevated *interleukin 1 beta* mRNA expression, and enhanced reactive oxygen species production were also observed. In conclusion, our zebrafish model is simple, rapid, effective and affordable, incorporating key features of AD and aging, thus may become a unique and powerful tool for high-throughput screening of anti-AD compounds in vivo.

1. Introduction

Alzheimer's disease (AD) is an age-related and progressive neurodegenerative disease characterized by memory loss, cognitive deficits, and severe behavioral disturbances. AD has a prevalence of 10–30 % in individuals aged > 65 years. More than 90 % cases of AD are sporadic (onset >65 years) and less than 10 % of cases are familial (usually with an onset before 65 years of age) [1]. As the world's population is increasingly aging, the number of patients with AD is expected to reach 130 million worldwide by 2050, which will cause a heavy burden on the families and society as a whole [2]. The main hallmarks of AD are β-amyloid (Aβ) deposition in senile plaques, emergence of hyperphosphorylated tau protein in neurofibrillary tangles, and loss of cholinergic neurons in the basal forebrain. In addition, other factors, such as oxidative stress and neuroinflammation, are also involved in the pathogenesis of AD [3]. Due to the complex and incompletely understood etiology of AD, the currently approved drugs such as donepezil can only ameliorate some of the AD symptoms, but cannot prevent the progression of AD [4]. Many rodent models of AD have been intensively studied, providing a considerable insight into AD mechanisms. However, these models are relatively costly and take long time to develop, which slows down progress towards developing AD therapeutics [5-8]. Therefore, other inexpensive in vivo AD models with high-throughput screening capacity that can rapidly and efficiently identify more active and specific compounds with therapeutic potential are rather necessary.

Zebrafish (*Danio rerio*) has high biological, structural, functional, and genetic similarities with humans and is rapidly emerging as an attractive model for research on human diseases [9,10]. In addition, zebrafish is an excellent model for time- and cost-efficient high-throughput drug screening because of its small size, high fecundity, easy husbandry, and transparent embryonic and larval stages [11,12]. Many small molecules shown to have therapeutic activity in zebrafish have made it to clinical trials, e.g., leflunomide for the treatment of melanoma [13]. Several pharmacological models of AD in zebrafish, including those induced by aluminum trichloride ($AlCl_3$) [14], scopolamine [15], and okadaic acid [16], have been used to rapidly screen potential therapeutics for AD. Notably, aluminum represents an environmental risk factor for AD, as toxic effects of water, food, and other sources contaminated by aluminum have been linked to an increase in AD occurrence [17,18]. Aluminum easily crosses the blood-brain barrier and accumulates in the brain, especially in the frontal cortex and hippocampus [19]. Exposure to $AlCl_3$ causes cholinergic dysfunction, Aβ accumulation,

* Corresponding authors.
E-mail addresses: yanglefmmu@163.com (L. Yang), minggao@fmmu.edu.cn (M. Zhao).

https://doi.org/10.1016/j.csbj.2024.05.036
Received 17 February 2024; Received in revised form 4 May 2024; Accepted 21 May 2024
Available online 22 May 2024

neuroinflammation, oxidative stress, and ultimately affects memory and learning both in rodents and zebrafish [20-22]. Previous studies reported that daily exposure to appropriate concentrations of $AlCl_3$ for 3–5 days could successfully induce an AD-like pathology in zebrafish. Accordingly, some potential anti-AD compounds such as linarin [23] and trihydroxy piperlongumine [24] were discovered in the zebrafish model of AD induced by $AlCl_3$. Therefore, $AlCl_3$ is an appropriate and efficient agent to induce AD-like manifestations in zebrafish.

Although various genetic and environmental factors have been demonstrated to be linked to the development of AD, the single greatest risk factor of that condition is age [25]. Increasing evidence suggests that gradual accumulation of pathological changes during normal aging likely contributes to the cognitive impairments observed in older individuals. The aging brain commonly harbors different pathological features, some of which are AD-related pathologies [25]. In particular, cellular senescence may be an important factor in AD pathophysiology, so senolytic therapies, e.g., a combination of dasatinib and quercetin, may be as an attractive alternative strategy in AD treatment [26,27]. D-galactose (D-gal) is known to induce brain aging owing to the conversion of D-gal into aldose and hydrogen peroxide, resulting in increased reactive oxygen species (ROS) levels [28]. Chronic administration of D-gal at low doses was shown to induce changes that mimic natural aging processes in animals, including cognitive impairment, oxidative stress, increased inflammatory response, as well as gene transcriptional alterations [28,29]. Therefore, when $AlCl_3$ is used to model AD in young animals, its combination with D-gal may better simulate AD-like symptoms in the elderly. Previous studies have shown that a combination of D-gal and $AlCl_3$ induces changes in rodents that resemble natural aging, e.g., memory impairment, hair loss, humped back, as well as AD-like features, such as deficits in the cholinergic system, expression of high levels of Aβ proteins, oxidative stress, and inflammation [5,30,31]. However, the rodent AD models have limitations, such as high cost of housing and suboptimal suitability for large-scale screening.

In the present study, in order to overcome some shortcomings of the rodent AD models, we attempted to establish a new AD model in zebrafish by a combined treatment with $AlCl_3$ and D-gal at different concentrations. The behavioral performance parameters, such as learning and memory, response ability, and locomotor capacity were evaluated by the plus-maze and light/dark test. Moreover, we investigated the main hallmarks of AD and aging to determine whether the AD model in zebrafish was successfully established.

2. Results

2.1. Effects of co-treatment with $AlCl_3$ and D-gal at different doses on learning and memory

To explore the optimal combination of $AlCl_3$ and D-gal concentrations to cause learning and memory impairments, we first determined the maximum tolerance concentration by evaluating the mortality of zebrafish from exposure to three different concentrations of $AlCl_3$ (160, 180 and 200 μM) in combination with 51.2 mg/mL D-gal at 2 days post-fertilization (dpf) for 72 h. Results showed that 5 dpf zebrafish mortality increased significantly with the increase in $AlCl_3$ concentration. Notably, when the concentration of $AlCl_3$ reached 200 μM, all zebrafish in the study perished (Fig. S1). Therefore, we reduced $AlCl_3$ and D-gal concentrations and used combinations of 60, 80, 100, or 140 μM $AlCl_3$ with 25.6 mg/mL D-gal. We found that zebrafish subjected to any of these four combined treatments showed long survival and good physical condition. Moreover, the learning and memory ability of zebrafish after exposure to these combined treatments was evaluated using the plus-maze test, a color preference assay based on zebrafish showing an innate preference for blue over other colors [32]. The four experimental zebrafish groups did not show any significant difference in the total distance swam in the blue region compared to that in the control group (Fig. S2), suggesting that at these concentrations, $AlCl_3$ and D-gal did not impair learning and memory in zebrafish.

Based on these results, we further adjusted the concentrations of $AlCl_3$ and D-gal and used the following five combinations: 150 μM $AlCl_3$ + 30 mg/mL D-gal, 150 μM $AlCl_3$ + 40 mg/mL D-gal, 200 μM $AlCl_3$ + 20 mg/mL D-gal, 200 μM $AlCl_3$ + 30 mg/mL D-gal, and 200 μM $AlCl_3$ + 40 mg/mL D-gal. All zebrafish exposed to these five combinations survived and moved normally. Based on this, we further evaluated the performance of the zebrafish in learning and memory tests. As shown in Fig. 1, except for the group treated with 150 μM $AlCl_3$ + 30 mg/mL D-gal, zebrafish treated with the remaining four combinations moved significantly less in the blue region than did control zebrafish, indicating that co-administration of these four doses of $AlCl_3$ and D-gal significantly dysregulated learning and memory in zebrafish (Fig. 1).

2.2. Effects of co-treatment with $AlCl_3$ and D-gal at different doses on response ability

Zebrafish larvae show a clear and distinct pattern of swimming movement in response to light and dark conditions. This swimming behavior is strongly linked to social interaction, anxiety, learning and memory, and defense [33]. In the present study, we evaluated the response ability of zebrafish under alternating light-dark stimulation. In the control group, the movement speed was fast in the dark environment and slow in the bright environment (Fig. 2**A**), which was reflected in the large difference between relative speeds per minute in the bright and dark environments (Fig. 2**B**). After co-treatment with the five combinations of $AlCl_3$ and D-gal described in the previous paragraph, the speed change in the light and dark compartments (Fig. 2**A, B**) as well as the total distance swam (Fig. 2**C, D**) significantly decreased. These results indicated that co-administration of $AlCl_3$ and D-gal weakened the response ability and locomotor capacity of zebrafish. Taking into account the results of the plus-maze test, we concluded that learning and memory, response ability, and locomotion were significantly impaired upon exposure to the following four combinations of $AlCl_3$ and D-gal: 150 μM $AlCl_3$ + 40 mg/mL D-gal, 200 μM $AlCl_3$ + 20 mg/mL D-gal, 200 μM $AlCl_3$ + 30 mg/mL D-gal, and 200 μM $AlCl_3$ + 40 mg/mL D-gal. Therefore, subsequent experiments were carried out using these four combinations.

2.3. Effects of co-treatment with $AlCl_3$ and D-gal at different doses on acetylcholinesterase activity

Acetylcholinesterase (AChE), an important enzyme responsible for acetylcholine hydrolysis in the brain and inducing cholinergic neuronal dysfunction, is currently the primary target of AD therapy [34]. Therefore, after treatment with different doses of $AlCl_3$ and D-gal at 2 dpf for 72 h, we determined the AChE activity of 5 dpf zebrafish to confirm successful construction of an AD model. We found that the fluorescence intensity associated with a product of enzymatic reaction catalyzed by AChE in zebrafish treated with the four selected combinations of $AlCl_3$ and D-gal was significantly higher compared to that in the normal control group (Fig. 3**A**). This finding aligns with the observed behavioral performance of zebrafish as discussed above.

2.4. Effects of co-administration of $AlCl_3$ and D-gal on $A\beta_{1-42}$ plaques

Aβ deposition is an important clinical hallmark in patients with AD. We next examined the level of $A\beta_{1-42}$, a highly neurotoxic amyloid peptide that accumulates in the brains of patients with AD [35]. As shown in Fig. 3B, only few $A\beta_{1-42}$ plaques were observed in the control group. In contrast, there was a notable increase in the content of $A\beta_{1-42}$ plaques observed in zebrafish treated with any of the selected four combinations of $AlCl_3$ and D-gal (Fig. 3**B**). This increasing trend was consistent with the increase in AChE activity, suggesting that exposure to these four combinations of $AlCl_3$ and D-gal may induce AD-like

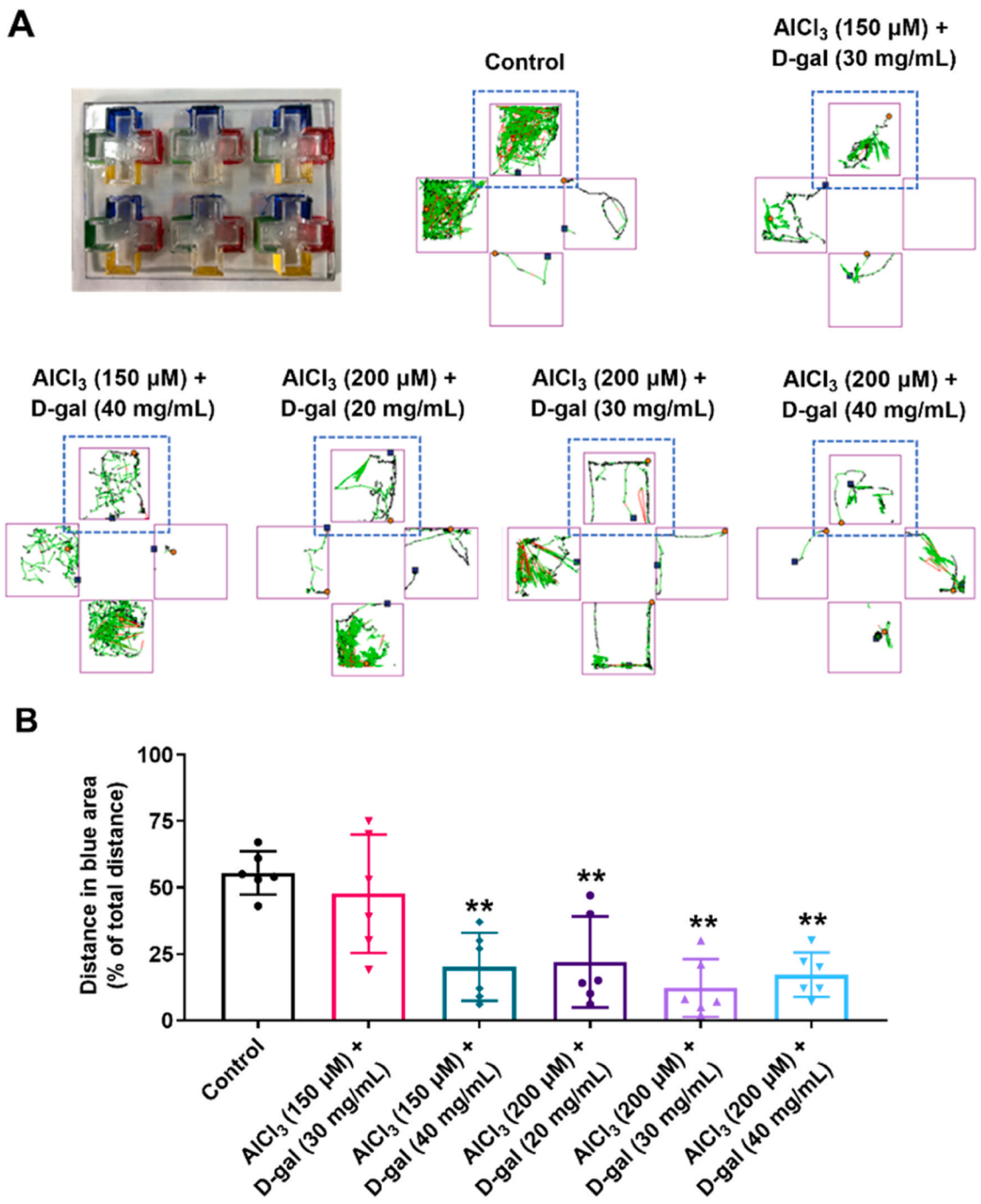

Fig. 1. Assessment of color-associated learning and memory in the plus-maze test. **A**: Schematic diagram of plus-maze and representative swimming trajectories in the plus-maze test. **B**: Quantitative analysis of the ratio of distance swam in the blue area to the total distance swam in 2 dpf zebrafish after exposure to four different combinations of $AlCl_3$ and D-gal for 72 h. Data are presented as the mean ± SEM ($n = 30$ zebrafish larvae per group), and the distance of five zebrafish represents one data point. Statistical significance of treatment effects was assessed using one-way ANOVA with Dunnett's multiple comparison test and illustrated as follows: * * $p < 0.01$ (versus the control group).

manifestations in zebrafish.

2.5. *Effects of co-treatment with $AlCl_3$ and D-gal at of different doses on the levels of β-galactosidase and telomerase activities*

The levels of senescence-associated β-galactosidase and telomerase activity are commonly used as cell aging biomarkers [36]. The β-galactosidase activity in the 200 μM $AlCl_3$ + 20 mg/mL D-gal treatment group showed no significant difference from that in the control group **(**Fig. 4**A, B)**. However, co-treatment with other three combinations of $AlCl_3$ and D-gal dramatically increased β-galactosidase activity **(**Fig. 4**A, B)**. In contrast, we found that telomerase activity in all four treatment groups were about twofold lower than that in the control group **(**Fig. 4**C)**. These results indicate that exposure to the combinations of 150 μM $AlCl_3$ + 40 mg/mL D-gal, 200 μM $AlCl_3$ + 30 mg/mL D-gal, or 200 μM $AlCl_3$ + 40 mg/mL D-gal induced significant aging features in zebrafish.

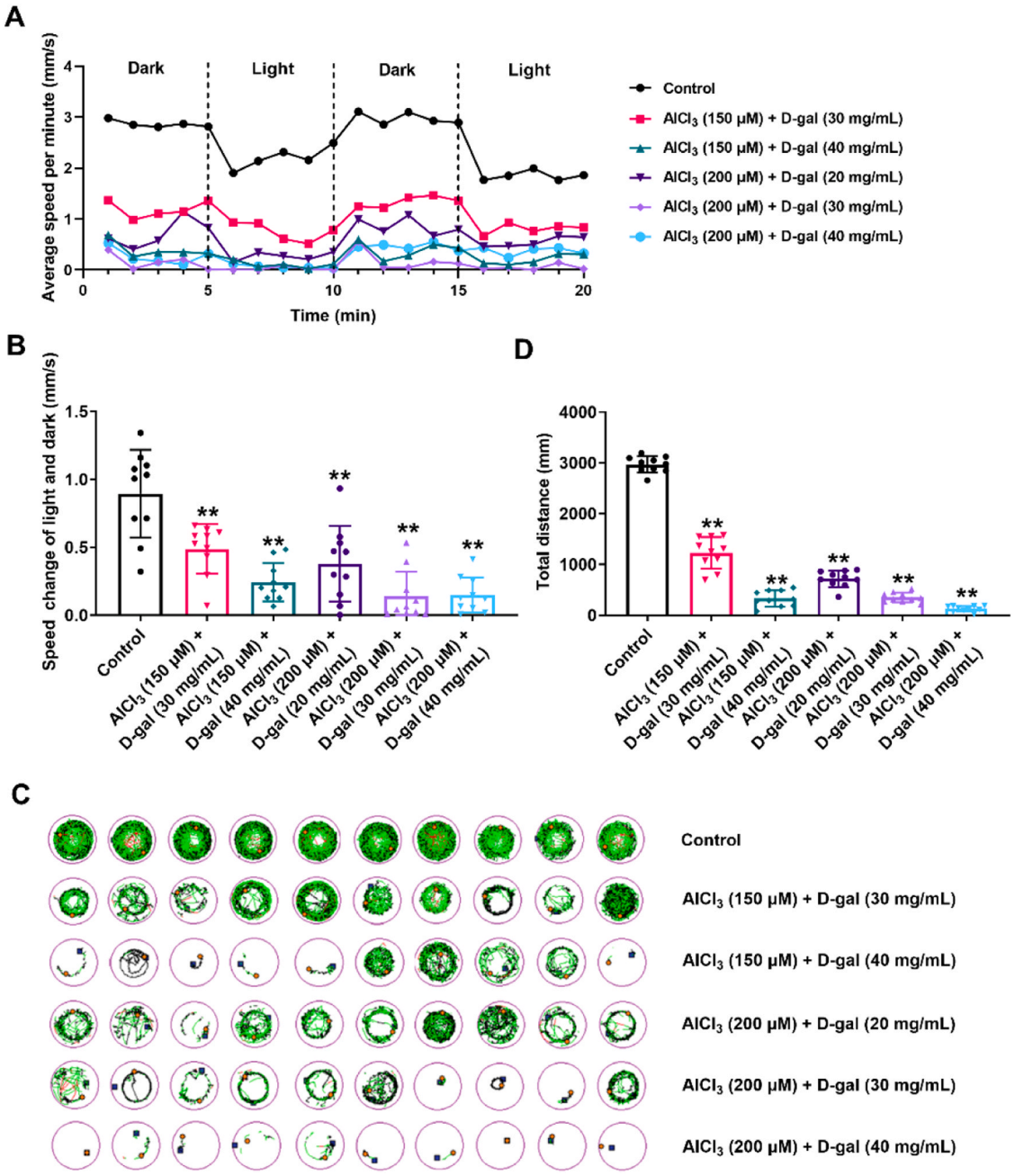

Fig. 2. Assessment of the response ability and locomotor behavior in the light-dark test. **A**: Locomotor patterns and average speed during dark-light stimulations of zebrafish after exposure to four different combinations of $AlCl_3$ and D-gal from 2 to 5 dpf. **B**: Quantitative analysis of the average speed change during light-dark stimulations. **C**: Representative traces of total locomotor activity in different groups during all light-dark stimulations. **D**: Quantitative analysis of total distance swam during all light-dark stimulations. In **B** and **D**, data are presented as the mean ± SEM ($n = 10$ zebrafish larvae per group). Statistical significance of treatment effects was assessed using one-way ANOVA with Dunnett's multiple comparison test and illustrated as follows: * * $p < 0.01$ (versus the control group).

2.6. Effects of co-treatment with $AlCl_3$ and D-gal at different doses on il1b mRNA expression

Inflammation is a hallmark of aging and driver of multiple age-related diseases such as AD [37]. Age-related build-up of senescent cells in the brain might be responsible for creating the perfect pro-inflammatory conditions to favor the onset of AD in the presence of other risk factors [27]. Interleukin 1 beta is one of the most common pro-inflammatory markers, and we found that *il1b* mRNA expression in each treatment group was about twofold higher than that in the control group **(**Fig. 5**A)**, suggesting that notable inflammation was induced by the four used combinations of $AlCl_3$ + D-gal.

2.7. Effects of co-treatment with $AlCl_3$ and D-gal at different doses on the ROS level

Oxidative stress plays a key role in the progression of aging and AD. Furthermore, overproduction of ROS results in oxidative stress [38]. Therefore, we further investigated the impact $AlCl_3$ and D-gal at different doses on oxidative stress in zebrafish using an oxidation-sensitive probe (CM-H2DCFDA) to measure ROS production. We found that fluorescence intensity of ROS in the 200 μM $AlCl_3$ + 20 mg/mL D-gal group was similar to that in the control group **(**Fig. 5**B)**. However, exposure of zebrafish to other three combinations of $AlCl_3$ + D-gal markedly increased ROS fluorescence intensity **(**Fig. 5**B)**,

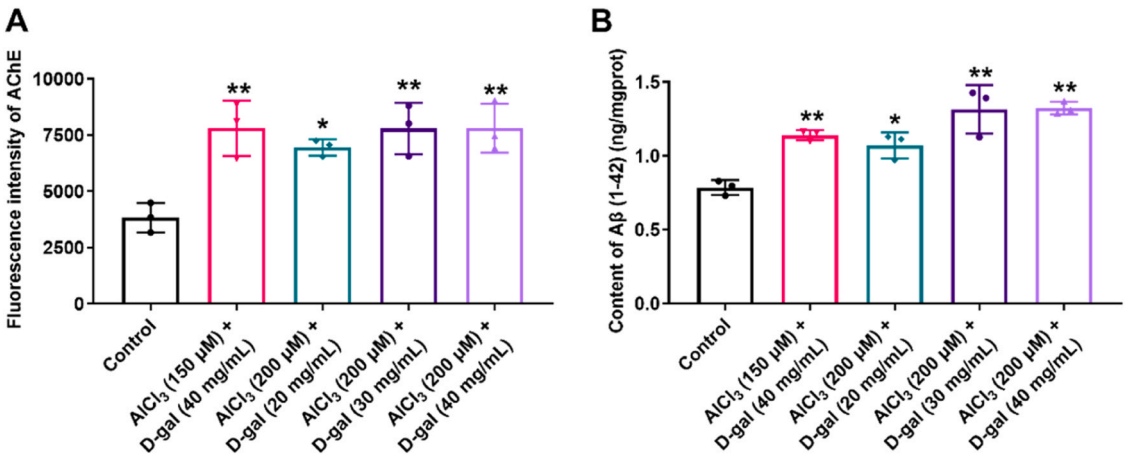

Fig. 3. Determination of AChE activity and $A\beta_{1-42}$ content. **A, B**: Quantitative analysis of AChE fluorescence intensity **(A)** and $A\beta_{1-42}$ plaques **(B)** after exposure of 2 dpf zebrafish to four combinations of $AlCl_3$ and D-gal for 72 h. Data are presented as the mean ± SEM ($n = 3$). Statistical significance of treatment effects was assessed using one-way ANOVA with Dunnett's multiple comparison test and illustrated as follows: * $p < 0.05$, * * $p < 0.01$ (versus control group).

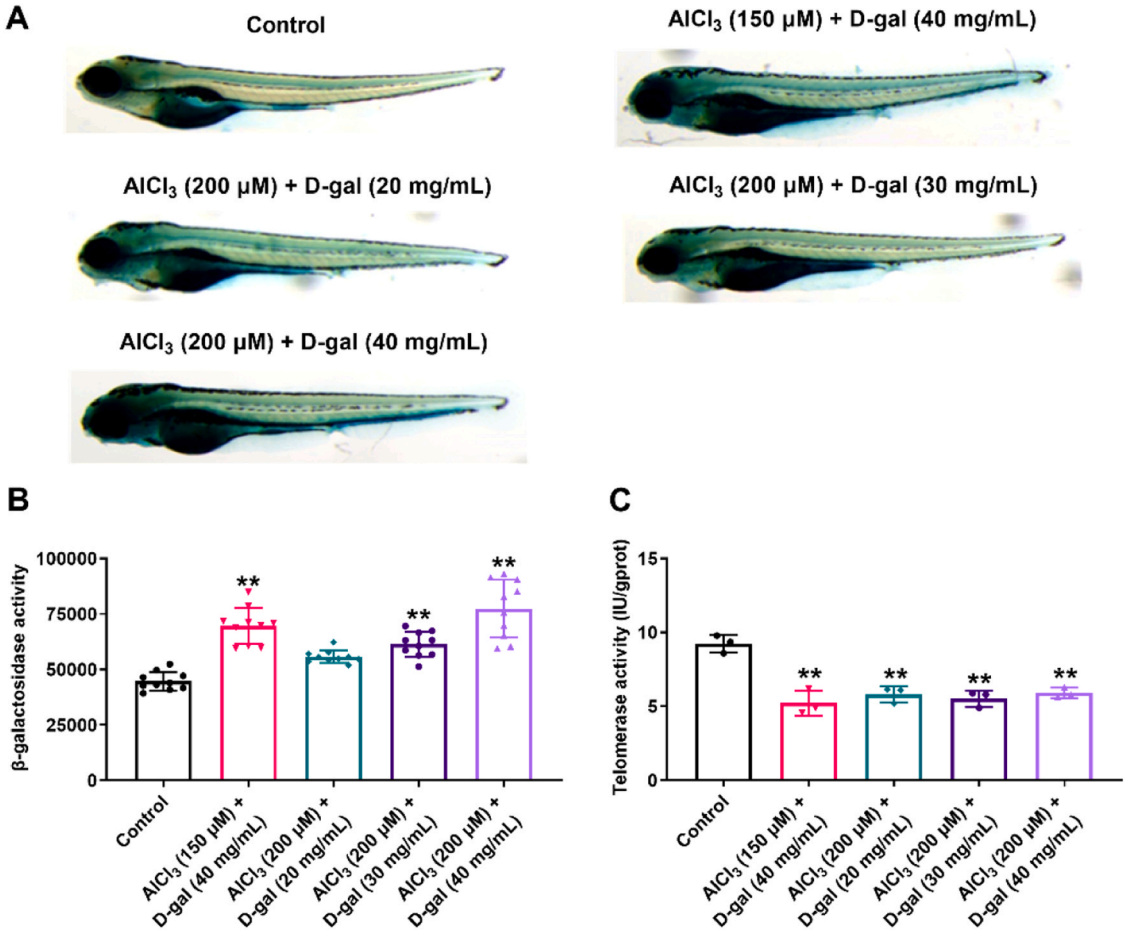

Fig. 4. Determination of β-galactosidase and telomerase levels. **A**: Representative images of staining for β-galactosidase. **B**, **C**: Quantitative analysis of β-galactosidase (**B**) and telomerase (**C**) activities after exposure of 2 dpf zebrafish to four different combinations of $AlCl_3$ and D-gal for 72 h. Data are presented as the mean ± SEM ($n = 10$ in **B** and n = 3 in **C**). In **B** and **C**, statistical significance of treatment effects was assessed using one-way ANOVA with Dunnett's multiple comparison test and illustrated as follows: * * $p < 0.01$ (versus control group).

indicating that co-treatment with those three combinations of $AlCl_3$ and D-gal significantly increased the ROS level.

3. Discussion

At present, there is an urgent need to develop an in vivo model of AD with high-throughput screening capacity that can rapidly and efficiently identify more active anti-AD compounds with therapeutic potential.

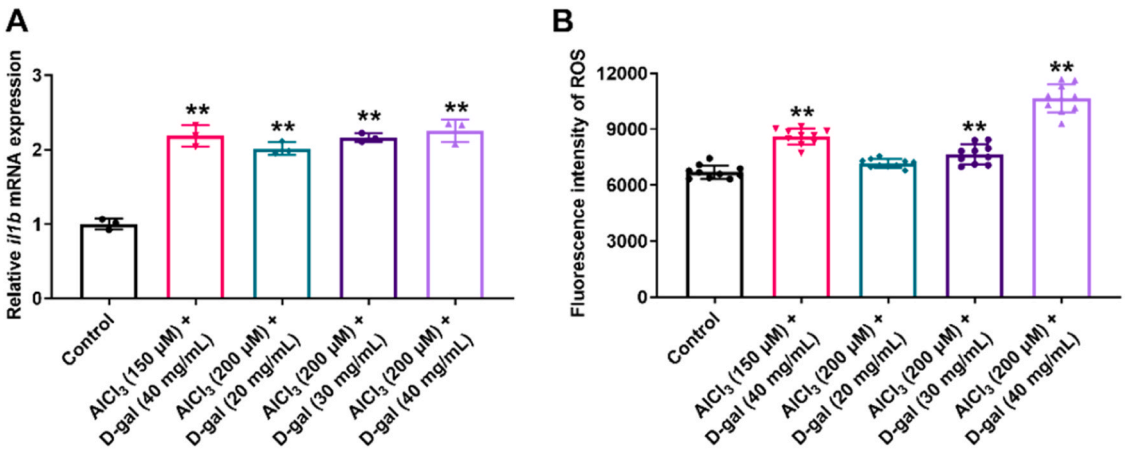

Fig. 5. Determination of *il1b* expression and ROS levels. **A**: Quantitative analysis of the relative *il1b* mRNA expression normalized by *actb1* mRNA level in 2 dpf zebrafish exposed to four combinations of $AlCl_3$ and D-gal for 72 h. **B**: Quantitative analysis of the fluorescence intensity of ROS levels after exposure of 2 dpf zebrafish to four different combinations of $AlCl_3$ and D-gal for 72 h. Data are presented as the mean ± SEM ($n = 3$ in **A** and $n = 10$ in **B**). Statistical significance of treatment effects was assessed using one-way ANOVA with Dunnett's multiple comparison test.

Owing to the small size, high fecundity, low cost, and transparency of the larvae, zebrafish larvae have been increasingly utilized in high-throughput behavioral analysis to discover potential therapeutically relevant compounds [39]. Aging is associated with a decline in cognitive performance, which is the biggest risk factor for the development of AD [25]. Both normal aging and AD are associated with overlapping and increased levels of pathology [25]. Despite several studies have described the usefulness of $AlCl_3$ as a common toxic agent to induce AD model in zebrafish, but in those models, symptoms of aging are difficult to simulate. In addition, D-gal is an accepted drug for accelerating aging, and studies have reported that combining D-gal with $AlCl_3$ in rodents can induce both aging and AD-like characteristics. However, the establishment of these rodent AD models usually takes 8–12 weeks [5,40,41], and our study also found that mice exposed to different doses of $AlCl_3$ and D-gal for 4 weeks showed no notable difference in locomotor and memory abilities, and significant impairments were observed after 10 weeks (Fig. S3). Therefore, in the current study, we constructed a zebrafish model of AD after co-treatment with $AlCl_3$ and D-gal from 2 dpf to 5 dpf, which has not been reported previously. This model combines AD-associated pathology and natural aging signs, and is simple, rapid, effective and affordable, enabling for screening a large number of anti-AD compounds in zebrafish.

A wide range of complex behaviors observed in mammalian models, including learning and memory, aggression, anxiety, social interaction, object discrimination, color and place preference have been comprehensively classified and characterized in zebrafish [42]. Therefore, different behavioral tests such as the T/Y-maze test, novel object recognition test, light-dark test and novel diving test were used to evaluate cognitive abilities, locomotion, exploratory tendencies, and anxiety in this zebrafish AD model [12]. Zebrafish have rich color vision, which is a distinct advantage over the rodent models. The majority of the behavioral assays are based on color discrimination and involves visual stimuli (either rewarding or aversive) used as cues for learning in zebrafish. Buatois et al., [43]. Due to its relative simplicity and ease, color preference screening using zebrafish larvae is suitable for high-throughput screening applications. Zebrafish larvae have been reported to show an innate preference for the blue color rather than for the red, green or yellow color in the T-maze and plus-maze tests [44]. Natural color preference is a major factor by which learning, memory, decision-making, and functionality of the zebrafish visual system can be assayed [45,46]. Therefore, we first investigated the effects of different combinations of $AlCl_3$ and D-gal using a plus-maze with four differently colored arms (red, yellow, blue, and white), and used the ratio of movement in the blue area to the total movement as an evaluative index for learning and memory impairment in this study. The results showed that zebrafish in all four experimental groups showed a significant decrease in the proportion of distance swam within the blue area, suggesting that the learning and memory function was obviously impaired. Sang et al. reported that zebrafish exposed to $AlCl_3$ (140 μM) from 2 to 5 dpf exhibited obvious dyskinesia and reduced response efficiency [47,48]. Similarly, these four combinations of $AlCl_3$ and D-gal in our study also significantly impaired the response ability and locomotor capacity of zebrafish larvae, as was observed in the light-dark test. These behavioral changes in zebrafish were similar to those previously described in mice and rats treated with $AlCl_3$ and D-gal [5,49].

Acetylcholine is an important cholinergic neurotransmitter for learning and memory, and its concentration in the synaptic cleft is regulated by AChE activity [34]. Pharmacological inhibition of AChE by drugs such as donepezil is currently considered as classic clinical treatment for AD. In addition, Aβ peptides in the brain play a key role in AD pathogenesis. The aggregation of Aβ peptides, particularly of $Aβ_{1–42}$, a key subtype with a higher neuronal toxicity and accumulation rate than those of $Aβ_{1–40}$, initiates the pathogenic cascade and ultimately leads to neuronal dysfunction and dementia [35]. Therefore, increased activity of AChE and $Aβ_{1–42}$ deposition are two important hallmarks of AD. Sun et al. reported that in a zebrafish AD model induced by $AlCl_3$ (80 μM) from 3 to 6 dpf, increased AChE activity and large Aβ plaques in the brain of AD zebrafish were observed [14]. Previous studies reported that combined administration of $AlCl_3$ and D-gal significantly increase AChE activity and $Aβ_{1–42}$ deposition in mice and rats, causing the development of learning and memory impairments [49,50]. Similarly, our findings showed that the combinations of $AlCl_3$ and D-gal that induced an obvious cognitive deficit and impaired response ability and locomotion in zebrafish also significantly increased the activity of AChE and $Aβ_{1–42}$ deposition. These results imply that the four different combinations of $AlCl_3$ and D-gal used in our experiments can be successfully utilized to establish an AD model in zebrafish.

Aging is a natural process characterized by a progressive functional decline of tissues, organs, and organ systems that leads to an increased susceptibility to age-related diseases and, ultimately, to death [25]. β-Galactosidase is a biomarker of aging, and its activity increases with advancing age in both zebrafish and humans [51,52]. The activity of telomerase, another marker of cellular aging, decreases with age, and such decline has been associated also with aging-related diseases. Environmental factors, including diet and lifestyle, affect the rate of telomere shortening, which can be reversed by telomerase [53]. In zebrafish, telomerase expression increases during the development between larval and juvenile stages, continues during young adulthood, and

subsequently declines at older ages [54]. A significant increase in β-galactosidase activity and a significant decrease in telomerase activity were observed in rodent models of aging induced by treatment with D-gal [55,56]. Additionally, although rodent models of AD induced by administration of $AlCl_3$ and D-gal replicate the aging process and induce AD-like symptoms, there are few studies on the biochemical indicators related to aging. In the present study, we found that β-galactosidase activity was dramatically increased after treatment with three different combinations of $AlCl_3$ and D-gal, whereas telomerase activity was significantly decreased in all treatment groups. Based on these results, we concluded that our zebrafish AD model induced by the combinations of 150 μM $AlCl_3$ + 40 mg/mL D-gal, 200 μM $AlCl_3$ + 30 mg/mL D-gal, or 200 μM $AlCl_3$ + 40 mg/mL D-gal showed obvious changes in aging biomarker. Therefore, compared with the characteristics of the previously described zebrafish AD model induced by $AlCl_3$ alone, our zebrafish larval AD model additionally emphasizes the aging process and therefore may better simulate the symptoms of elderly AD patients.

There is considerable evidence that inflammation and oxidative stress are important hallmarks of aging and drivers of multiple age-related diseases, such as AD [57]. The levels of oxidative stress and inflammation are well established to be increased in the brain of patients with AD [58]. D-gal is a reductive monosaccharide that stimulates excess production of ROS and advanced glycation end products, leading to oxidative stress, mitochondrial dysfunction, and inflammatory responses [28,29]. D-gal shortens life spans of mice with cognitive impairments and neurodegeneration associated with aging symptoms by increasing oxidative stress and inflammatory response [29]. Exposure to $AlCl_3$ also causes neuroinflammation and oxidative stress, and ultimately affects memory and learning both in rodents and zebrafish [20,21]. Previous studies reported that different combinations of $AlCl_3$ and D-gal increase generation of pro-inflammatory factors such as IL-1β and IL-6, as well as enhance production of oxidative stress factors such as ROS in rodents ([59,60]). In line with this, our results showed that the *il1b* mRNA expression and ROS levels were significantly increased in zebrafish exposed to different combinations of $AlCl_3$ and D-gal. These changes were in accord with altered fish behavior and changes in other biomarkers discussed above, further supporting the notion that this treatment can be used to successfully establish a valid AD model in zebrafish.

In conclusion, our study demonstrated that 2 dpf zebrafish exposed to several combinations of 150 μM $AlCl_3$ + 40 mg/mL D-gal, 200 μM $AlCl_3$ + 30 mg/mL D-gal, or 200 μM $AlCl_3$ + 40 mg/mL D-gal for 72 h reliably develop AD-like symptoms and manifest aging features. This zebrafish AD model showed significant learning and memory deficits and impairments in response ability and locomotion. Importantly, there is a strong synergistic effect of $AlCl_3$ and D-gal on cognitive impairment than that by $AlCl_3$ (150 or 200 μM) or D-gal (30 or 40 mg/mL) alone (**Fig. S4**). Furthermore, some typical biochemical features of AD and aging were observed, such as increased AChE and β-galactosidase activities, $A\beta_{1-42}$ deposition, reduced levels of telomerase, augmented *il1b* mRNA expression, and enhanced ROS production. Presence of other known AD pathologies, such as neurofibrillary tangles of hyperphosphorylated tau protein and mitochondrial dysfunction, should be explored in this model in the future. In summary, we have established a new zebrafish AD model that is simple, rapid, effective and low-cost, which may helpful in understanding mechanisms of AD, as well as in high-throughput screening of potential anti-AD compounds.

4. Materials and Methods

4.1. Zebrafish maintenance

Wild-type AB strain zebrafish larvae at 2 dpf used in this study were obtained from a commercial supplier (Hunter Biotechnology Co., LTD, Hangzhou, China, License number: SYXK (Zhejiang) 2022–0004). Zebrafish embryos were produced through natural pairwise mating conducted within our aquaculture facility. Only embryos that developed normally and reached appropriate stages were chosen for experiments. Zebrafish were kept at 28 °C in aerated water (200 mg instant ocean sea salt L^{-1}; conductivity: 450–550 μS/cm; pH: 6.5–8.5; hardness: 50.0–100.0 mg/L $CaCO_3$). All experiments were conducted in accordance with the Association for Assessment and Accreditation of Laboratory Animal Care International (AAALAC, 001458) and Institutional Animal Care and Use Committee (IACUC-2023–6463-01) guidelines.

4.2. Establishment of zebrafish AD model

D-galactose (D-gal, J2126173) and aluminum chloride ($AlCl_3$, C1628001) were purchased from Aladdin Biochemical Technology Co., Ltd (Shanghai, China). Stock solutions of D-gal (160 mg/mL) and $AlCl_3$ (50 mM) were prepared using 1 × E3 medium (5 mM NaCl, 0.17 mM KCl, 0.33 mM $CaCl_2$, 0.33 mM $MgSO_4$), diluted as needed, and prepared on demand. The majority of zebrafish developmental processes occur within the first day, and they hatch at 2 dpf [61]. Thus, 2 dpf zebrafish were chosen to establish the model. The 2 dpf larval zebrafish were randomly allocated into 6-well microplates at a density of 30 per well. Then they were co-treated with different doses of water-soluble D-gal and $AlCl_3$ (Fig. 1 **and S1**) from 2 to 5 dpf at a temperature of 28 ℃ to establish a zebrafish model of AD. The normal control group was also established, with each well containing 3 mL of fluid that was refreshed daily.

4.3. Color-associated learning and memory test (plus-maze test)

Behavioral tests were performed on zebrafish larvae at 5 dpf. The plus-maze tank had four identical arms designed in the shape of a cross that were painted in four different colors (yellow, blue, red and green; see Fig. 1**A** for the schematic diagram), as previously reported [32]. Zebrafish inherently incline to swim towards blue color, therefore displaying increased activity in the blue arm. However, this tendency is diminished during cognitive impairment [44]. The distance swam by zebrafish in each of the four regions within 10 min was recorded by an automated computerized video-tracking system (V3.11, ViewPoint Life Sciences, France). Each group contained 30 zebrafish, and five zebrafish were randomly selected to be placed in the maze at a time. The total distance swam by these five zebrafish in the blue zone and the total distance in all four zones were recorded, so each group contained six data points. The ratio of the distance swam in the blue compartment to that swam in the whole maze was used to evaluate the learning and memory ability of zebrafish.

4.4. Response ability assessment and locomotor test (light-dark test)

To evaluate the response ability and locomotion of zebrafish, the light-dark test was conducted as previously described [32,62]. After exposure to D-gal and $AlCl_3$ for 72 h, zebrafish at 5 dpf were distributed into 96-well plates, with one fish per well. The zebrafish were acclimated for 15 min before the motility recording. The tests were completed in 20 min, containing two cycles of dark/light phases (5 min of darkness and 5 min of light, alternately). The total distance swam in 20 min and speed changes during light-dark stimulations were recorded by a video-tracking system for further analysis.

4.5. Determination of AChE activity

After the behavioral studies, the concentrations of $AlCl_3$ + D-gal that caused significant cognitive and response impairment in zebrafish were selected to further evaluate the effects on AChE activity. Zebrafish at 5 dpf were euthanized by freezing using liquid nitrogen. Cold physiological saline was added to the larvae at a ratio of 1:9 (mass:volume), homogenized using automated tissue homogenization, and centrifuged at 2500 rpm for 10 min. The supernatant was collected for the

determination of AChE activity by using an Amplite™ Fluorimetric Acetylcholinesterase Assay Kit (2760191, AAT Bioquest, Pleasanton, CA, USA) according to the manufacturer's instructions [14]. The fluorescence at excitation and emission wavelengths of 490 and 525 nm was monitored using a Spark multimode microplate reader (Tecan, Austria).

4.6. Determination of $A\beta_{1-42}$ content

The $A\beta_{1-42}$ content was determined using a Zebrafish $A\beta_{1-42}$ ELISA kit (202308, Shanghai Enzyme Linked Biotechnology Co., Ltd, China) according to the manufacturer's instructions. Briefly, zebrafish at 5 dpf were euthanized by freezing using liquid nitrogen. Cold physiological saline was added to the larvae in a 1.5 mL tube at a ratio of 1:9 (mass: volume), homogenized, and centrifuged at 5000 × *g* for 10 min. The supernatant was collected for the assay. Absorbance was measured at 450 nm using a Spark multimode microplate reader (Tecan). The $A\beta_{1-42}$ concentrations are presented as ng/mg total protein.

4.7. Determination of β-galactosidase activity

Briefly, after exposure to D-gal and $AlCl_3$ for 72 h, zebrafish at 5 dpf in 6-well microplates were washed with 0.01 M phosphate buffered solution (PBS) 3 times, and β-galactosidase activity was detected using a cell senescence β-galactosidase staining kit (091821220526, Beyotime Biotechnology, China) following the manufacturer's instructions. After staining, 10 zebrafish from each experimental group were randomly selected and photographed under an anatomical microscope (SZX7, Olympus, Japan). Data were collected using NIS-Elements D 3.20 advanced image processing software to analyze the intensity of β-galactosidase staining in zebrafish.

4.8. Determination of telomerase activity

The telomerase activity was detected using a Zebrafish TE ELISA Kit (H23Y07, Shanghai Hengyuan Biotechnology Co., Ltd, China) following the manufacturer's instructions. The sample preparation method was the same as that for the $A\beta_{1-42}$ content detection. Absorbance was measured at 450 nm using a Spark multimode microplate reader (Tecan). The enzyme activity is presented as IU/g total protein.

4.9. Determination of interleukin 1 beta mRNA expression

Zebrafish at 5 dpf were euthanized by freezing using liquid nitrogen. The total RNA was extracted from the homogenized larval tissue using a Universal RNA Extraction TL Kit C (Foshan Aowei Biological Technology Co., Ltd, China) according to the manufacturer's instructions. Next, 2 μg of total RNA from each sample was reverse transcribed into cDNA using a FastKing cDNA first chain synthesis kit (X0320, Tiangen Biomedical Technology Co., Ltd., Beijing, China). The RT-qPCR was conducted using the iTaq Universal SYBR Green Supermix (1725124, Bio-rad, USA). The relative expression of the *il1b* gene was calculated using the $2^{-\triangle\triangle Ct}$ method, with *beta 1 actin* as reference gene. The primer sequences of the above genes are as follows：.

Genes	Primer sequence	
beta 1 actin	Forward	5′-TCGAGCAGGAGATGGGAACC-3′
	Reverse	5′-CTCGTGGATACCGCAAGATTC-3′
interleukin 1 beta	Forward	5′-GAACAGAATGAAGCACATCAAACC-3′
	Reverse	5′-ACGGCACTGAATCCACCAC-3′

4.10. Determination of ROS levels

The whole-embryo ROS levels were measured using a 5,6-chloromethyl-2′,7′-dichloro-dihydrofluorescein diacetate ROS assay kit (CM-H_2DCFDA, 2505981, Invitrogen, USA). At 2 dpf, zebrafish were randomly allocated into a 6-well microplate at a density of 30 zebrafish per well and co-treated with water-soluble D-gal and $AlCl_3$ at different concentrations at a temperature of 28 ℃. Each well contained 3 mL ROS fluorescent detection solution, and the solution was changed daily. After 72 h of treatment, zebrafish in each group were transferred to a black 96-well enzyme plate with two fish/well and a capacity of 100 μL/well. The ROS fluorescence at excitation and emission wavelengths of 484 and 535 nm was detected using a Spark multimode microplate reader (Tecan).

4.11. Statistical analysis

Data analysis was conducted using Prism 8.0 software (GraphPad Software, San Diego, CA, USA). Data are presented as the mean ± standard error of the mean (SEM) for at least three independent experiments. Statistical comparisons of multiple groups were done using one/two-way analysis of variance (ANOVA) followed by the Dunnett's multiple comparison test. Effects of treatments were considered significant if $p < 0.05$.

Author statement

All authors have read the revised manuscript and agree to submit it.

CRediT authorship contribution statement

Li Luo: Conceptualization, Data curation, Funding acquisition, Investigation, Methodology, Writing – original draft. **Tao Yan:** Data curation, Investigation, Methodology. **Le Yang:** Formal analysis, Supervision, Writing – review & editing. **Minggao Zhao:** Conceptualization, Project administration.

Declaration of Competing Interest

There are no conflicts of interest to declare.

Data Availability

All data generated or analyzed in this study are included in the article and supporting files.

Acknowledgements

This work was supported by the Key Research and Development Projects of Shaanxi Province, China (2020SF-142) and the National Natural Science Foundation of China (82304473).

Appendix A. Supporting information

Supplementary data associated with this article can be found in the online version at doi:10.1016/j.csbj.2024.05.036.

References

[1] Piaceri I, Nacmias B, Sorbi S. Genetics of familial and sporadic Alzheimer's disease. Front Biosci (Elite Ed) 2013;5(1):167–77. https://doi.org/10.2741/e605.
[2] Thakral S, Yadav A, Singh V, Kumar M, Kumar P, Narang R, Sudhakar K, Verma A, Khalilullah H, Jaremko M, Emwas AH. Alzheimer's disease: Molecular aspects and treatment opportunities using herbal drugs. Ageing Res Rev 2023;88:101960. https://doi.org/10.1016/j.arr.2023.101960.
[3] Monteiro AR, Barbosa DJ, Remiao F, Silva R. Alzheimer's disease: Insights and new prospects in disease pathophysiology, biomarkers and disease-modifying drugs. Biochem Pharm 2023;211:115522. https://doi.org/10.1016/j.bcp.2023.115522.
[4] Khan S, Barve KH, Kumar MS. Recent Advancements in Pathogenesis, Diagnostics and Treatment of Alzheimer's Disease. Curr Neuropharmacol 2020;18(11): 1106–25. https://doi.org/10.2174/1570159×18666200528142429.
[5] Chiroma SM, Mohd Moklas MA, Mat Taib CN, Baharuldin MTH, Amon Z. d-galactose and aluminium chloride induced rat model with cognitive impairments. Biomed Pharm 2018;103:1602–8. https://doi.org/10.1016/j.biopha.2018.04.152.

[6] Oddo S, Caccamo A, Shepherd JD, Murphy MP, Golde TE, Kayed R, Metherate R, Mattson MP, Akbari Y, LaFerla FM. Triple-transgenic model of Alzheimer's disease with plaques and tangles: intracellular Abeta and synaptic dysfunction. Neuron 2003;39(3):409–21. https://doi.org/10.1016/s0896-6273(03)00434-3.
[7] Puzzo D, Gulisano W, Palmeri A, Arancio O. Rodent models for Alzheimer's disease drug discovery. Expert Opin Drug Discov 2015;10(7):703–11. https://doi.org/10.1517/17460441.2015.1041913.
[8] Puzzo D, Gulisano W, Palmeri A, Arancio O. Rodent models for Alzheimer's disease drug discovery. Expert Opin Drug Dis 2015;10(7):703–11. https://doi.org/10.1517/17460441.2015.1041913.
[9] Chia KL, Klingseisen A, Sieger D, Priller J. Zebrafish as a model organism for neurodegenerative disease. Front Mol Neurosci 2022:940484. https://doi.org/10.3389/fnmol.2022.940484.
[10] Kalueff AV, Stewart AM, Gerlai R. Zebrafish as an emerging model for studying complex brain disorders. Trends Pharm Sci 2014;35(2):63–75. https://doi.org/10.1016/j.tips.2013.12.002.
[11] Patton EE, Zon LI, Langenau DM. Zebrafish disease models in drug discovery: from preclinical modelling to clinical trials. Nat Rev Drug Discov 2021;20(8):611–28. https://doi.org/10.1038/s41573-021-00210-8.
[12] Wang XB, Zhang JB, He KJ, Wang F, Liu CF. Advances of Zebrafish in Neurodegenerative Disease: From Models to Drug Discovery. Front Pharm 2021;12:713963. https://doi.org/10.3389/fphar.2021.713963.
[13] White RM, Cech J, Ratanasirintrawoot S, Lin CY, Rahl PB, Burke CJ, Langdon E, Tomlinson ML, Mosher J, Kaufman C, Chen F, Long HK, Kramer M, Datta S, Neuberg D, Granter S, Young RA, Morrison S, Wheeler GN, Zon LI. DHODH modulates transcriptional elongation in the neural crest and melanoma. Nature 2011;471(7339):518–22. https://doi.org/10.1038/nature09882.
[14] Sun C, Zhang S, Ba S, Dang J, Ren Q, Zhu Y, Liu K, Jin M. Eucommia ulmoides Olive Male Flower Extracts Ameliorate Alzheimer's Disease-Like Pathology in Zebrafish via Regulating Autophagy, Acetylcholinesterase, and the Dopamine Transporter. Front Mol Neurosci 2022;15:901953. https://doi.org/10.3389/fnmol.2022.901953.
[15] Boiangiu RS, Mihasan M, Gorgan DL, Stache BA, Hritcu L. Anxiolytic, promnesic, anti-acetylcholinesterase and antioxidant effects of cotinine and 6-hydroxy-l-nicotine in scopolamine-induced zebrafish (danio rerio) model of Alzheimer's disease. Antioxid (Basel) 2021;10(2). https://doi.org/10.3390/antiox10020212.
[16] Koehler D, Williams FE. Utilizing zebrafish and okadaic acid to study Alzheimer's disease. Neural Regen Res 2018;13(9):1538–41. https://doi.org/10.4103/1673-5374.237111.
[17] Campbell A. The potential role of aluminium in Alzheimer's disease. Nephrol Dial Transpl 2002;17(Suppl 2):17–20. https://doi.org/10.1093/ndt/17.suppl_2.17.
[18] Rahman MA, Rahman MS, Uddin MJ, Mamum-Or-Rashid ANM, Pang MG, Rhim H. Emerging risk of environmental factors: insight mechanisms of Alzheimer's diseases. Environ Sci Pollut Res Int 2020;27(36):44659–72. https://doi.org/10.1007/s11356-020-08243-z.
[19] Fernandes RM, Correa MG, Aragao WAB, Nascimento PC, Cartagenes SC, Rodrigues CA, Sarmiento LF, Monteiro MC, Maia C, Crespo-Lopez ME, Lima RR. Preclinical evidences of aluminum-induced neurotoxicity in hippocampus and prefrontal cortex of rats exposed to low doses. Ecotoxicol Environ Saf 2020;206:111139. https://doi.org/10.1016/j.ecoenv.2020.111139.
[20] Dey M, Singh RK. Chronic oral exposure of aluminum chloride in rat modulates molecular and functional neurotoxic markers relevant to Alzheimer's disease. Toxicol Mech Methods 2022;32(8):616–27. https://doi.org/10.1080/15376516.2022.2058898.
[21] Kaur K, Narang RK, Singh S. AlCl(3) induced learning and memory deficit in zebrafish. Neurotoxicology 2022;92:67–76. https://doi.org/10.1016/j.neuro.2022.07.004.
[22] Nie Y, Yang J, Zhou L, Yang Z, Liang J, Liu Y, Ma X, Qian Z, Hong P, Kalueff AV, Song C, Zhang Y. Marine fungal metabolite butyrolactone I prevents cognitive deficits by relieving inflammation and intestinal microbiota imbalance on aluminum trichloride-injured zebrafish. J Neuroinflamm 2022;19(1):39. https://doi.org/10.1186/s12974-022-02403-3.
[23] Pan HY, Zhang JH, Wang YY, Cui KK, Cao YT, Wang LH, Wu YJ. Linarin improves the dyskinesia recovery in Alzheimer's disease zebrafish by inhibiting the acetylcholinesterase activity. Life Sci 2019;222:112–6. https://doi.org/10.1016/j.lfs.2019.02.046.
[24] Haridevamuthu B, Raj D, Kesavan D, Muthuraman S, Kumar RS, Mahboob S, Al-Ghanim KA, Almutairi BO, Arokiyaraj S, Gopinath P, Arockiaraj J. Trihydroxy piperlongumine protects aluminium induced neurotoxicity in zebrafish: Behavioral and biochemical approach. Comp Biochem Physiol C Toxicol Pharm 2023;268:109600. https://doi.org/10.1016/j.cbpc.2023.109600.
[25] Keller JN. Age-related neuropathology, cognitive decline, and Alzheimer's disease. Ageing Res Rev 2006;5(1):1–13. https://doi.org/10.1016/j.arr.2005.06.002.
[26] Gonzales MM, Garbarino VR, Kautz TF, Palavicini JP, Lopez-Cruzan M, Dehkordi SK, Mathews JJ, Zare H, Xu P, Zhang B, Franklin C, Habes M, Craft S, Petersen RC, Tchkonia T, Kirkland JL, Salardini A, Seshadri S, Musi N, Orr ME. Senolytic therapy in mild Alzheimer's disease: a phase 1 feasibility trial. Nat Med 2023. https://doi.org/10.1038/s41591-023-02543.
[27] Guerrero A, De Strooper B, Arancibia-Cárcamo L. Cellular senescence at the crossroads of inflammation and Alzheimer's disease. Trends Neurosci 2021;44(9):714–27. https://doi.org/10.1016/j.tins.2021.06.007.
[28] Pantiya P, Thonusin C, Ongnok B, Chunchai T, Kongkaew A, Nawara W, Arunsak B, Chattipakorn N, Chattipakorn SC. Chronic D-galactose administration induces natural aging characteristics, in rat's brain and heart. Toxicology 2023;492:153553. https://doi.org/10.1016/j.tox.2023.153553.
[29] Azman KF, Zakaria R. D-Galactose-induced accelerated aging model: an overview. Biogerontology 2019;20(6):763–82. https://doi.org/10.1007/s10522-019-09837-y.
[30] Xiao F, Li XG, Zhang XY, Hou JD, Lin LF, Gao Q, Luo HM. Combined administration of D-galactose and aluminium induces Alzheimer-like lesions in brain. Neurosci Bull 2011;27(3):143–55. https://doi.org/10.1007/s12264-011-1028-2.
[31] Zhang Z, Wu H, Qi S, Tang Y, Qin C, Liu R, Zhang J, Cao Y, Gao X. 5-Methyltetrahydrofolate alleviates memory impairment in a rat model of Alzheimer's Disease Induced by D-Galactose and Aluminum Chloride. Int J Environ Res Public Health 2022;19(24). https://doi.org/10.3390/ijerph192416426.
[32] Guo S, Zhang X, Zhang Y, Chen X, Zhang Y, Cao B, Xia D. Development of a rapid zebrafish model for lead poisoning research and drugs screening. Chemosphere 2023;345. https://doi.org/10.1016/j.chemosphere.2023.140561.
[33] Basnet RM, Zizioli D, Taweedet S, Finazzi D, Memo M. Zebrafish larvae as a behavioral model in neuropharmacology. Biomedicines 2019;7(1). https://doi.org/10.3390/biomedicines7010023.
[34] Ferreira-Vieira TH, Guimaraes IM, Silva FR, Ribeiro FM. Alzheimer's disease: Targeting the Cholinergic System. Curr Neuropharmacol 2016;14(1):101–15. https://doi.org/10.2174/1570159×13666150716165726.
[35] Hardy J, Selkoe DJ. The amyloid hypothesis of Alzheimer's disease: progress and problems on the road to therapeutics. Science 2002;297(5580):353–6. https://doi.org/10.1126/science.1072994.
[36] Boccardi V, Pelini L, Ercolani S, Ruggiero C, Mecocci P. From cellular senescence to Alzheimer's disease: The role of telomere shortening. Ageing Res Rev 2015;22:1–8. https://doi.org/10.1016/j.arr.2015.04.003.
[37] Zhao Y, Simon M, Seluanov A, Gorbunova V. DNA damage and repair in age-related inflammation. Nat Rev Immunol 2023;23(2):75–89. https://doi.org/10.1038/s41577-022-00751-y.
[38] Ionescu-Tucker A, Cotman CW. Emerging roles of oxidative stress in brain aging and Alzheimer's disease. Neurobiol Aging 2021;107:86–95. https://doi.org/10.1016/j.neurobiolaging.2021.07.014.
[39] Lessman CA. The developing zebrafish (Danio rerio): a vertebrate model for high-throughput screening of chemical libraries. Birth Defects Res C Embryo Today 2011;93(3):268–80. https://doi.org/10.1002/bdrc.20212.
[40] Li H, Kang T, Qi B, Kong L, Jiao Y, Cao Y, Zhang J, Yang J. Neuroprotective effects of ginseng protein on PI3K/Akt signaling pathway in the hippocampus of D-galactose/AlCl3 inducing rats model of Alzheimer's disease. J Ethnopharmacol 2016;179:162–9. https://doi.org/10.1016/j.jep.2015.12.020.
[41] Zhang Y, Pi Z, Song F, Liu Z. Ginsenosides attenuate d-galactose- and AlCl(3)-inducedspatial memory impairment by restoring the dysfunction of the neurotransmitter systems in the rat model of Alzheimer's disease. J Ethnopharmacol 2016;194:188–95. https://doi.org/10.1016/j.jep.2016.09.007.
[42] Rosa JGS, Lima C, Lopes-Ferreira M. Zebrafish Larvae Behavior Models as a Tool for Drug Screenings and Pre-Clinical Trials: A Review. Int J Mol Sci 2022;23(12):6647. https://doi.org/10.3390/ijms23126647.
[43] Buatois A, Nguyen S, Bailleul C, Gerlai R. Colored-light preference in zebrafish (Danio rerio). Zebrafish 2021;18(4):243–51. https://doi.org/10.1089/zeb.2020.1977.
[44] Park JS, Ryu JH, Choi TI, Bae YK, Lee S, Kang HJ, Kim CH. Innate Color Preference of Zebrafish and Its Use in Behavioral Analyses. Mol Cells 2016;39(10):750–5. https://doi.org/10.14348/molcells.2016.0173.
[45] Avdesh A, Martin-Iverson MT, Mondal A, Chen M, Askraba S, Morgan N, Lardelli M, Groth DM, Verdile G, Martins RN. Evaluation of color preference in zebrafish for learning and memory. J Alzheimers Dis 2012;28(2):459–69. https://doi.org/10.3233/JAD-2011-110704.
[46] Jia L, Raghupathy RK, Albalawi A, Zhao Z, Reilly J, Xiao Q, Shu X. A colour preference technique to evaluate acrylamide-induced toxicity in zebrafish. Comp Biochem Physiol C Toxicol Pharm 2017;199:11–9. https://doi.org/10.1016/j.cbpc.2017.01.004.
[47] Sang ZP, Wang KR, Han X, Cao MX, Tan ZH, Liu WM. Design, synthesis, and evaluation of novel ferulic acid derivatives as multi-target-directed ligands for the treatment of Alzheimer's Disease. Acs Chem Neurosci 2019;10(2):1008–24. https://doi.org/10.1021/acschemneuro.8b00530.
[48] Sang ZP, Wang KR, Shi J, Liu WM, Cheng XF, Zhu GF, Wang YL, Zhao YY, Qiao ZP, Wu AG, Tan ZH. The development of advanced structural framework as multi-target-directed ligands for the treatment of Alzheimer's disease. Eur J Med Chem 2020;192:112180. https://doi.org/10.1016/j.ejmech.2020.112180.
[49] Wei Y, Liu D, Zheng Y, Li H, Hao C, Ouyang W. Protective effects of kinetin against aluminum chloride and D-galactose induced cognitive impairment and oxidative damage in mouse. Brain Res Bull 2017;134:262–72. https://doi.org/10.1016/j.brainresbull.2017.08.014.
[50] Li ZP, Chen X, Lu WQ, Zhang S, Guan X, Li ZY, Wang D. Anti-oxidative stress activity is essential for mediated neuroprotection on glutamate-induced apoptotic HT22 Cells and an Alzheimer's Disease Mouse Model. Int J Mol Sci 2017;18(8):1623. https://doi.org/10.3390/ijms18081623.
[51] Kishi S, Bayliss PE, Uchiyama J, Koshimizu E, Qi J, Nanjappa P, Imamura S, Islam A, Neuberg D, Amsterdam A, Roberts TM. The identification of zebrafish mutants showing alterations in senescence-associated biomarkers. PLoS Genet 2008;4(8):e1000152. https://doi.org/10.1371/journal.pgen.1000152.
[52] Kishi S, Uchiyama J, Baughman AM, Goto T, Lin MC, Tsai SB. The zebrafish as a vertebrate model of functional aging and very gradual senescence. Exp Gerontol 2003;38(7):777–86. https://doi.org/10.1016/s0531-5565(03)00108-6.
[53] Tsoukalas D, Fragkiadaki P, Docea AO, Alegakis AK, Sarandi E, Thanasoula M, Spandidos DA, Tsatsakis A, Razgonova MP, Calina D. Discovery of potent telomerase activators: Unfolding new therapeutic and anti-aging perspectives. Mol Med Rep 20(4), 3701-3708 2019. https://doi.org/10.3892/mmr.2019.10614.

[54] Anchelin M, Murcia L, Alcaraz-Perez F, Garcia-Navarro EM, Cayuela ML. Behaviour of telomere and telomerase during aging and regeneration in zebrafish. PLoS One 2011;6(2):e16955. https://doi.org/10.1371/journal.pone.0016955.
[55] Li J, Zhang YC, Chen G. Effect of Ginkgo biloba Extract EGb761 on Hippocampal Neuronal Injury and Carbonyl Stress of D-Gal-Induced Aging Rats. Evid Based Complement Altern Med 2019;2019:5165910. https://doi.org/10.1155/2019/5165910.
[56] Saafan SM, Mohamed SA, Noreldin AE, El Tedawy FA, Elewa YHA, Fadly RS, Al Jaouni SK, El-Far AH, Alsenosy AA. Rutin attenuates D-galactose-induced oxidative stress in rats' brain and liver: molecular docking and experimental approaches. Food Funct 2023;14(12):5728–51. https://doi.org/10.1039/d2fo03301a.
[57] Leyane TS, Jere SW, Houreld NN. Oxidative stress in ageing and chronic degenerative pathologies: molecular mechanisms involved in counteracting oxidative stress and chronic inflammation. Int J Mol Sci 2022;23(13). https://doi.org/10.3390/ijms23137273.
[58] Namioka N, Hanyu H, Hirose D, Hatanaka H, Sato T, Shimizu S. Oxidative stress and inflammation are associated with physical frailty in patients with Alzheimer's disease. Geriatr Gerontol Int 2017;17(6):913–8. https://doi.org/10.1111/ggi.12804.
[59] Hu Y, Fang X, Wang J, Ren TT, Zhao YY, Dai JF, Qin XY, Lan R. Astragalin attenuates AlCl(3)/D-galactose-induced aging-like disorders by inhibiting oxidative stress and neuroinflammation. Neurotoxicology 2022;91:60–8. https://doi.org/10.1016/j.neuro.2022.05.003.
[60] Zhao H, Liu J, Wang Y, Shao M, Wang L, Tang W, Wang Y, Li X. Polysaccharides from sea buckthorn (Hippophae rhamnoides L.) berries ameliorate cognitive dysfunction in AD mice induced by a combination of d-gal and AlCl(3) by suppressing oxidative stress and inflammation reaction. J Sci Food Agric 2023;103(12):6005–16. https://doi.org/10.1002/jsfa.12673.
[61] Gatto E, Bruzzone M, Lucon-Xiccato T. Innate visual discrimination abilities of zebrafish larvae. Behav Process 2021;193:104534. https://doi.org/10.1016/j.beproc.2021.104534.
[62] Kim SS, Hwang KS, Yang JY, Chae JS, Kim GR, Kan H, Jung MH, Lee HY, Song JS, Ahn S, Shin DS, Lee KR, Kim SK, Bae MA. Neurochemical and behavioral analysis by acute exposure to bisphenol A in zebrafish larvae model. Chemosphere 2020;239:124751. https://doi.org/10.1016/j.chemosphere.2019.124751.